

Contents lists available at ScienceDirect

Separation and Purification Technology

journal homepage: www.elsevier.com/locate/seppur



Extraction of valuable chemicals from food waste via computational solvent screening and experiments

Yagya Gupta a,b, Souryadeep Bhattacharyya b, Dionisios G. Vlachos b, Vlachos

- ^a Department of Chemical & Biomolecular Engineering, University of Delaware, 150 Academy St., Newark, DE 19716, U.S.A
- b Catalysis Center for Energy Innovation, RAPID Manufacturing Institute, and Delaware Energy Institute (D.E.I.), University of Delaware, 221 Academy St., Newark, DE 19716, U.S.A

ARTICLE INFO

Keywords: Food waste Extraction Process intensification COSMO-RS HSPiP Solvent selection

ABSTRACT

About 1.3 billion tons of global food production end up in landfills and composting, leading to significant anthropogenic greenhouse gas (GHG) emissions. Extracting antioxidant and antimicrobial chemicals (flavonoids, phenolic acids, etc.) from food waste is an economically lucrative valorization strategy but is hindered by efficient solvent selection. Here we perform in silico high throughput screening to identify high solubility solvents for key phenolics and reveal >100+ higher-performing solvents than the traditional ethanol and methanol. Solubilities of nine shortlisted solvents are measured and found in reasonable agreement with model predictions. Analysis of the Conductor like Screening Model for Real Solvents (COSMO-RS) σ -profiles and Hansen Solubility Parameters reveals that polarity and hydrogen bonding make dimethylformamide (DMF) an excellent single solvent. We showcase the replacement of high-solubility toxic solvents with green mixtures and demonstrate the approach to potato peel waste. Our work provides a blueprint for solvent selection and generates new insights into extraction from food waste.

1. Introduction

Food waste (FW) is a grand challenge fueled by ineffective or partial waste management, overconsumption in developed countries, and increasing food production. An estimated 1.3 billion tons (~1/3 of the globally produced food) end up annually as waste during harvesting, transportation, processing, distribution, and consumption [1,2]. About half of the globally grown fruits, vegetables, roots, and tubers are wasted at the retail and consumer level [2]. Aside from the loss of resources, FW also leads to greenhouse gas (GHG) emissions [3]. The US landfills are the third-largest anthropogenic source of methane, which, along with composting, account for 34% of global anthropogenic GHG emissions [4]. The current management methods include anaerobic digestion [5], composting [6], fermentation [7], and animal feed. These methods are not economically, environmentally, and socially lucrative due to producing low-value products (biogas, ethanol, compost), GHG emissions, and long processing times (up to a few months).

An alternative is to shift from a linear economy (production, distribution, consumption, and disposal) into a circular one by repurposing FW to higher-value products, motivated by legislation [8] and sustainability drivers of the United Nations [9] by valorizing the key FW

components (carbohydrates, proteins, extractives, lipids, and lignin). Thermal and catalytic valorization methods involve hydrolysis [10], gasification [14], pyrolysis [12], hydrothermal processing [13], catalytic conversion of carbohydrates [12], fats and oils [14], depolymerization of the lignin [15], and extraction of the bioactive compounds. Lipids can be upgraded to fuels and lubricants, carbohydrates to biopolymers and dietary supplements, lignin to phenolics, and proteins to amino acids for food preservatives, dietary supplements, biopolymers, and cosmetics. Most current processing schemes are harsh and produce small molecules rather than high-value compounds.

In a recent review [16], we highlighted high-value extractives that should be recovered first before any harsh thermochemical processing. For example, phenolic acids, such as gallic, vanillic, and *p*-coumaric acid, will make a \$7.4 billion antioxidant industry by 2031 [17]. Even though the extractives vary among feedstocks (Table 1), hydroxycinnamic acids, flavonoids, and carotenoids exist in most feedstocks and are value-added for the pharmaceutical, cosmetic, and food industries. The ten key extractives commonly found in most food commodities and their market size are listed in Table 2.

Prior work performed extraction from potato peels [16], bananas [18], apples [19], tomatoes [20], orange peels [21], grape seeds [22],

E-mail address: vlachos@udel.edu (D.G. Vlachos).

^{*} Corresponding author.

Table 1Volumes of food commodity waste and major extractives by weight percentage.

Food Commodity	Global Waste Volume (million tons)	Major Extractives	Weight Percentage (%)
Apple [72,73]	13	Flavonoids	2.10
		Chlorogenic	0.40
		acid	
Orange [74]	11	Quercetin	1.04
		Caffeic acid	0.30
		Kaempferol	0.50
Banana [75]	17	Flavonoids	0.10
		Sinapic acid	4×10^{-4}
		Ferulic acid	0.01
Tomato	10	Carotenoids	0.02
[76–78]		Phenolics	0.03
		Flavonoids	0.01
Olive [79,80]	20	Vanillic acid	0.01
		Caffeic acid	0.03
		α-tocopherol	0.02
Potato [81]	54	Chlorogenic	0.02
		acid	
		Carotenoids	1.9×10^{-4}
		Ascorbic acid	0.03
Mango [82]	8	Caffeic acid	0.10
		Gallic acid	0.02
		p-Coumaric	0.33
		acid	

using methanol, ethanol and water as solvents. These solvents are widely employed due to their high polarity, low boiling point, reasonable cost, and non-toxic properties. The high polarity facilitates the extraction of target polyphenols, and the low boiling point enables a less energy-intensive recovery of extractives. A vital consideration is their

safety for human consumption due to the application of target extractives in the pharmaceutical, cosmetic, and food industries. Thus, the choice of solvent is essential for enhancing selective extraction [23]. A comprehensive solvent evaluation for extraction of value-added chemicals from FW or other biomass sources has not been conducted to the best of our knowledge. Here, we focus on discovering an optimum solvent(s) for enhancing extraction efficiency. Given their accuracy (see below), computational tools are applied as estimation tools to guide our solvent selection and design of experiments. We introduce the ADF-COSMO-RS multiscale simulation software to identify top extraction solvents among 2000+ solvents, inspired by its application to liquid--liquid extraction for biorefinery platform chemicals, such as furfural and 5-hydroxymethyl furfural (HMF) [24,25]. Analysis of COSMOgenerated σ-profiles reveals that polarity and hydrogen bonding are critical for enhanced solubility. The predicted top nine green or yellow solvents are then experimentally assessed. Since extracted target compounds are used mainly in the pharmaceutical and food industry, purity and greenness are crucial. Thus, we propose replacing high-performing but toxic solvents with high-solubility green solvent mixtures using the Hansen Solubility Parameters in Practice (HSPiP) software. We demonstrate our approach to potato peel waste. Our study provides a blueprint for solvent selection and generates new insights into extracting compounds from FW.

2. Materials and experimental methods

2.1. Materials

Vanillic acid (HPLC grade (purity \geq 97%)), caffeic acid (HPLC grade

Table 2
Commercially important extractives (name and structure) in FW feedstocks and market size (2020–2021).

Extractives	Structure	Market Size (USD, in million dollars)	
Ascorbic acid [83]	HO HO O	\$953.8	
Gallic acid [84]	но он	\$71	
Vanillic acid [85]	но он он	\$1200	
Chlorogenic acid (CGA) [87]	HO, CO2H	\$132.2	
p-Coumaric acid	он Он	Part of the CGA market	
Ferulic acid [88]	HO CH ₃	\$68	
Caffeic acid	но	Part of the CGA market	
Quercetin [89]	но	\$261 (part of the flavonoids market)	
Kaempferol [90]	но	\$3740	
β-carotene [86]	OH JOH	\$436.67	

(purity \geq 98%)), and quercetin (HPLC grade (purity \geq 95% purity)) were purchased from Sigma Aldrich. *p*-Coumaric acid (purity 98%), chlorogenic acid (purity 99.45%), and ferulic acid (purity 99.4%) were purchased from Fisher Scientific. ASTM-Type 1 grade deionized (DI) water (Milli-Q ® Direct) was used in all experiments. Solvents N,N-dimethylformamide (HPLC grade (purity \geq 99.9%)), 2,4,6-trimethylpyridine (G.C. grade (purity \geq 99%)), cyclohexanone (ACS reagent (purity \geq 99%)), cyclohexanol (G.C. grade (purity \geq 98.5%)), 4-methyl-2-pentanone (MIBK) (HPLC grade (purity \geq 99.5%)), dimethyl sulfoxide (anhydrous with purity \geq 99.9%), 2-propanol (HPLC grade (purity 99.9%)), ethanol (ACS reagent (purity \geq 99.5%)), and 2-pentanone (HPLC grade (purity 99.5%)) were obtained from Sigma Aldrich.

2.2. Quantification of compounds

The solubility was quantified using high-performance liquid chromatography (HPLC) using a Waters e2695 separations module coupled to a Waters 2414 refractive index meter and a Waters 2998 photodiode array detector. An Agilent Zorbax SB-C18, 250 mm column was used at 323 K, using a 50/50 (v/v) acetonitrile and water mixture flowing at 0.3 mL/min mobile phase. The solubility for acids was calculated from the area of their absorbance peak measured between 260 and 370 nm at their respective retention time (Supplementary Table 1).

The concentration of acids in the extraction from potato peel waste was quantified using liquid chromatography-mass spectrometry on a Q-orbitrap mass spectrometer (Supplementary Table 2). A Waters Acquity UPLC BEH C18 column (1.7 μm 2.1 X 30 mm) was used with solvent A: water containing 0.1% formic acid and solvent B: acetonitrile containing 0.1% formic acid as the mobile phase flowing at 0.5 mL/min. A gradient method was set up for 0% B to reach 95% B in 5 min.

2.3. Room temperature solubility measurements

The solubility measurements were conducted at room temperature (298 K), following the shake flask method suggested in the EPA protocol [26].

2.4. Estimation of an approximate solubility range

Initial experiments for every solute–solvent combination entailed 0.1 g of pure solute in 1 mL of solvent in a 20 mL scintillation vial at 303 K with constant stirring for 10 min. If the solution were clear, the solubility was ≥ 0.1 g/mL; otherwise, another 1 mL of solvent was added, and the vial was stirred for another 10 min. If the solids dissolved, the solubility was between 0.05 and 0.1 g/mL; otherwise, 8 mL of solvent was added and stirred for 24 h. If the solids are dissolved, the solubility is between 0.01 and 0.05 g/ml; otherwise, the solubility is < 0.01 g/ml.

2.5. Solubility experiments at 298 K

Excess solute (3 times over the screening solubility value) was added to 5 mL of solvent in three separate vials. All the vials were equilibrated at 303 K for 24 h at 1000 rpm followed by 24 h equilibration without stirring at 298 K. A saturated solution at 303 K ensures that dissolved solids would come out from the solvent phase at 298 K and accurate measurement of solubility. The equilibration time was determined by temporal studies on vanillic acid in ethanol and cyclohexanone and ferulic and p-coumaric acid in cyclohexanone. 3 h was deemed sufficient for equilibration, and 24 h ensured equilibration for all systems. The vial was centrifuged at 298 K for 10 min at 10,000 rpm. A clear solution was then quantified using HPLC.

2.6. Sample preparation

Different kinds of potatoes (russet, yellow, and yukon gold) were purchased from ACME, rinsed with water, and peeled uniformly with a manual peeler. Potato peels were also collected from the household kitchen to diversify the feedstock. The peels were dried under a vacuum oven at 333 K for 12 h to reduce the moisture content below 10 wt% based on the NREL LAP NREL/TP-510–42620 protocol [27]. The dried peels were grounded using a Thomas Wiley® Mini Cutting Mills to a powder of size $<0.5\,\mathrm{mm}$. The powder was stored at room temperature in an air-tight container. The Sartorius moisture content analyzer was used to determine the moisture content.

2.7. Soxhlet extraction from potato peel waste (PPW)

200 mL solvent was taken in a round bottom flask with 5 g of PPW in a thimble. The solvent was heated on reflux at its boiling point, allowing it to vaporize and condense to drop in the thimble until the solvent reached the siphon height, where it fell back into the round bottom flask (RBF). This process was conducted until the thimble's solvent appeared clear, indicating that the extraction has culminated. The RBF was cooled to room temperature, and the remaining solvent from the thimble was poured back into the flask. 200 mL of extracted solution was filtered and stored for the Total Phenolic Content (TPC) test. The solvent was vaporized on a rotary evaporator, and the RBF was weighed. The weight percentage of extraction from FW was calculated as follows:

Amount of extractives in RBF = weight of RBF after extraction - weight of RBF before extraction

Weight % Extractives =
$$\frac{amount\ of\ extractives}{5} \times 100$$

2.8. One-pot extraction from PPW

20~mL of solvent was taken in a round bottom flask and 1~g of PPW was added. Since methanol is a low boiling point solvent (64.7 $^{\circ}$ C), $60~^{\circ}$ C was selected as the extraction temperature to allow efficient contact between every solvent and solute. The mixture was heated to $60~^{\circ}$ C for 2~h. The solvent was then filtered and stored for quantification. Experiments were conducted in triplicates. A new PPW was also prepared to replace the two-year-old batch. Time-dependent extractions were performed from new PPW in DMF and methanol for 30~min to 10~h at $60~^{\circ}$ C and a 1:20~solid-to-liquid ratio. The solid-to-liquid (S:L) ratio was varied from 0.05~to 0.5~at $60~^{\circ}$ C for 4~h. Further, we recycled PPW and performed multiple extraction cycles using fresh solvent every time at $60~^{\circ}$ C and 1:5~S:L ratio for 4~h.

2.9. Total phenolic content (TPC) test

The total phenolic content in a sample was determined according to Ismail et al [28]. In summary, the gallic acid standards were prepared in DI water ranging from 0.02 to 0.64 mg/ml. The Folin-ciocalteau (FC) reagent was diluted 10-fold using DI water, and a 6 wt% of sodium bicarbonate was prepared. 0.75 mL of FC reagent was taken in a 20 mL scintillation vial, and 100 μL of the extract was added. The mixture was allowed to stand for 5 min, and then 0.75 mL of 6 wt% sodium bicarbonate was added. The mixture was vortexed and allowed to stand for 90 min. The calibration curve was prepared using gallic acid standards to obtain the gallic acid equivalent (GAE). The absorbance was read at 600 nm, and the results were expressed as milligrams (mg) of GAE per g of dried potato peel.

2.10. Computational methodology

Many thermodynamic models have been developed, such as group contribution methods (GCM), quantitative-structure property relationship (QSPR), and force-field models. GCMs, such as UNIFAC [29] and modified UNIFAC [30], cannot be applied to molecules with undefined functional groups or when the interaction parameters between functional groups are missing. These models can also not predict multiple

thermodynamic properties using the same parameter set. Monte Carlo (MC) and molecular dynamics (MD) simulations are computationally expensive for large molecules and unsuitable for screening as the force field may need tuning for each solvent. As an alternative, implicit continuum solvation theories, which treat the solvent as a homogeneous continuous polarizable medium characterized by its dielectric constant, can be used. The solvation energy is estimated fundamentally, i.e., the molecule is transferred from vacuum to a solvent medium, and one accounts for the long-range electrostatic free energy, cavity formation energy, and dispersion free energy. The COnductor like Screening MOdel for Real Solvents (COSMO-RS) utilizes this method and stands out in its ability to predict multiple thermodynamic properties without experimental data as opposed to CGMs.

2.11. COSMO-RS

The COSMO-RS optimizes the geometry of the molecule of interest in a vacuum using density functional theory (DFT). Then it performs a solvation calculation to determine the total energy when the solute is transferred from a vacuum to a perfect conductor. COSMO stores the screening charge density (SCD) surface of the molecule of interest in a database. For geometry optimization of the molecules to determine the lowest energy conformer, the TZP small-core basis set, the Becke-Perdew (GGA BP86) functional, and the scalar ZORA were used. Using the COSMO σ -profile, the distribution of SCD is created, where the screening charge surface is segmented into areas interacting with each other and the environment. This essentially forms the basis for estimating the interaction energy between pairs of surface segments. The misfit energy is zero when the surface segment consists of equal and opposite charges (perfectly screened); otherwise, an energy penalty proportional to the size of the surface segments and the square of the charge density difference is applied. Hydrogen bonding (HB) interactions are considered for surface segments carrying high surface charge densities. These interactions are a function of temperature as HB weakens at higher temperatures. These energy considerations bring the σ-profile into context to capture the distribution of the screening charge of the surfaces and enable the second COSMO-RS step of statistical mechanics calculations to estimate the chemical potential of a component. The mixture σ -profile is a weighted average of the pure component σ-profiles for an arbitrary number of components [31]. It is calculated as follows:

$$p_s(\sigma) = \frac{\sum_i x_i n_i p_i(\sigma)}{\sum_i x_i n_i}$$

where $p_s(\sigma)$ is mixture σ -profile, x_i is the mole fraction of molecule i, n_i is the total number of surface segments around the molecular cavity and $p_i(\sigma)$ is the probability of finding a segment with a surface charge density for molecule i.

In this work, in silico database screening of solubilities of 2,421 compounds is conducted using the ADF COSMO-RS implementation in the ADF2019.302 modeling suite with the ADFCRS-2018 database [32,33]. The solubilities are calculated at 303 K and 343 K (excluding ionic liquids) in the database. The inputs to COSMO-RS are compiled using literature and include the melting point, enthalpy of fusion, and change in heat capacity of the solid and subcooled liquid at the melting temperature (Supplementary Table 3) [34-51]. The COSMO-RS model and its implementation by ADF can be found elsewhere [52,53]. The accuracy of COSMO-RS is compromised due to the approximations regarding the acid dissociation factor, long-range interactions, and weak intermolecular forces [54]. It treats solvent as a continuum and does not account for discreet solvent-molecule interactions. Similarly, it considers the solute an ensemble of non-interacting molecules and underestimates long-range interactions. Consequently, it cannot accurately describe systems with multiple or geometrically arranged interactions, limiting its accuracy in strongly polar or HB systems [55]. Although useful for rapid screening, the underlying assumptions preclude

estimating green solvent mixtures to replace DMF. Thus, we employed Hansen Solubility Parameters to design mixtures that effectively capture the polar and HB forces crucial for target compounds' solvation. In addition, the conformational distribution also influences the thermodynamic properties; further work would be worthwhile in reducing the errors [56].

2.12. Green single and mixture solvent selection

A list of environmentally benign green and yellow solvents was compiled from the US Food and Drug Administration [57], Chem21 solvent selection guide [58], and pharmaceutical companies (GSK [59], Sanofi [60], and Pfizer [61]). These solvents are scored based on safety (boiling point, density, volatility, flash point, risk of peroxides, energy of decomposition), environmental (global warming potential, biodegradability, ecotoxicity, life cycle analysis), and health impact (acute, longterm, and organ toxicity) and specific industrial constraints to classify them as green, yellow, and red. Chem21 classifies solvents based on the listed criteria where safety accounts for flammability, the environmental score indexes the toxicity of the solvent to aquatic life, soil, and atmosphere, and the health score describes its occupational hazard. Sanofi includes quality, cost, and chemical efficiency beyond safety, environmental, and health issues. Since the definition of green solvents is subjective and varies among sources, we compiled these lists to identify 58 green and yellow solvents for our solubility study (Supplementary Table 4). Nine common green solvents that provide the highest solubility for the nine positively correlated key extractives are then identified, based on COSMO-RS solubility screening, and subsequently used for experimental verification of the predicted data.

2.13. HSPiP

The software HSPiP, which uses the Hansen Solubility Parameters (HSP) developed by Hansen [62] in 1967, was employed to identify green solvent mixtures to replace high solubility but rather toxic solvents. It has in-built data of the three HSP, i.e., dispersion (δD_1) , polar (δP_1) , and hydrogen bonding (HB) (δH_1) forces for 10,000+compounds. It can estimate the HSP using an artificial neural network (ANN) for unknown compounds from SMILES [63]. The HSP sphere concept can also be used to estimate the unknown HSP of a particular solute. The solvents are classified into good (score 1) and bad (score 0) based on whether they dissolve the solute. The coordinates of the center of the sphere are the HSP $(\delta D_1, \delta P_1, \delta H_1)$ of the solute. The radius of this sphere is R_0 . The distance (R_a) between a solvent and a solute provides their 'likeness':

$$R_a^2 = 4(\delta D_1 - \delta D_2)^2 + (\delta P_1 - \delta P_2)^2 + (\delta H_1 - \delta H_2)^2.$$

The smaller the distance, the more likely to be compatible. The relative energy difference (RED), defined as R_{a}/R_{o} , provides an estimate of how likely a solvent is to solubilize the solute with values between 0 and 1, signifying molecular similarity and high solubility.

HSPiP has an in-built solvent optimizer and a green solvent database and allows user-defined solvent lists to find an optimum solvent mixture. The target HSP of the solute or solvent is used to obtain the composition of the mixture (of two or three solvents) closest (minimum distance) to the target.

3. Results and discussion

In this work, we propose that solvent selection for extraction of bioactive compounds from FW or biomass should consider at least solubility, chemical reactivity, and toxicity. The solubility of target compounds is critical. The specified solvents are further screened for their chemical reactivity since by-products are undesirable. The list of green and yellow solvents encompasses important physical properties, such as flash point, freezing point, boiling point, density, volatility, refractive index, viscosity, etc., besides toxicity and safety discussed above. The

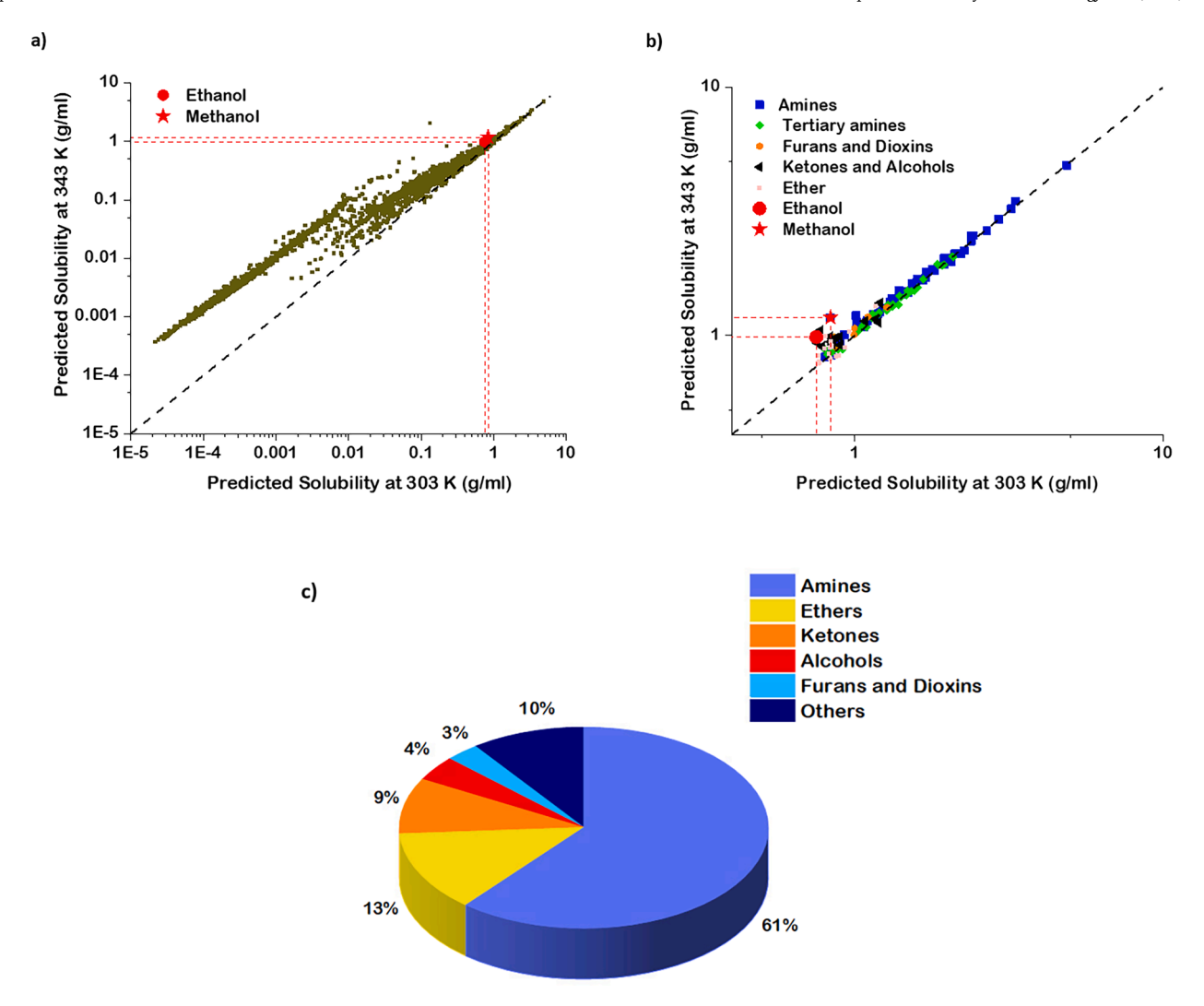


Fig. 1. a) COSMO-RS-predicted solubility for vanillic acid solubility at two common extraction temperatures 303 K and 343 K. b) Zoomed-in data for solvents better than ethanol and methanol grouped based on the functional groups. c) Distribution of different classes of 157 solvents.

following sections provide results and discussion on the proposed framework, with the first section presenting COSMO-RS and HSPiP prediction results on identifying top solvents for all target compounds. The second section offers an experimental assessment of the predicted results on selected green and yellow solvents and fundamental insights into solvent selection. The final section provides the application of the chosen solvent to potato peel waste and compares its performance with a traditional solvent toward the extraction of target phenolic acids.

3.1. COSMO-RS and HSPiP results

Ethanol, methanol, and their mixtures with water are the most common extraction solvents for biomass and FW. For vanillic acid, the ADF COMSO-RS predicts 130 and 156 (Supplementary Table 5) higher solubility solvents than methanol and ethanol, respectively (Fig. 1a). As expected, the solubility increases with temperature for most solvents, but the effect of temperature varies. The high-performing solvents contain different functionalities (Fig. 1b), with amines being the top and predominant (61%) in the list (Fig. 1c). Since the extracted compounds are acids, basic solvents have higher solubility due to reacting with the solute to a by-product. Tertiary amines constitute > 20% of the 157 solvents due to their high basicity. The best solvents are multi-functional polar compounds, such as 1-amino-2-propanol, acetoin, and 1-hexanamine, to name a few.

The solubility for all ten key extractives in 2400 + solvents yields a

matrix (Fig. 2a). The positive correlation among 9 of the 10 compounds (except β -carotene) suggests a similar solubility in the same solvent and simultaneous extraction from FW in a suitable solvent. HSPiP was further used to calculate the R_a of the solutes in the 2400 + solvents (Fig. 2b). The positive correlation among 9 out of 10 compounds affirms the qualitative agreement between these complementary tools.

The negative correlation between β -carotene and the other extractives stems from the molecular structures (Table 2). β -carotene is a bulky molecule with a long hydrocarbon chain that lacks the polar hydroxyl and carboxyl groups of the other compounds. This contrast in the physicochemical properties is also evidenced in the COSMO-RS σ -profiles (Fig. 2c). The σ profile of β -carotene (blue) is concentrated around σ (e/Ų) = 0, signifying a low polarity, consistent with its small polar and HB HSP values (0.83 and 1.9, respectively). The other compounds (Supplementary Table 6) have significant polarity ($\delta P > 7.56$) and HB character ($\delta H > 13.73$), congruent with the HB ability in the σ -profile (peaks at σ (e/Ų) > 0.0079 and σ (e/Ų) < -0.0079) and higher polarity (lower peaks at $\sigma=0$).

3.2. Experimental assessment

Out of the 100 + solvents, most solvents are either reactive or toxic. Thus, we have identified 58 green and yellow solvents based on various green solvent lists. Given the correlations of the extractives, one can focus on one of the nine and β -carotene. We down-selected the nine

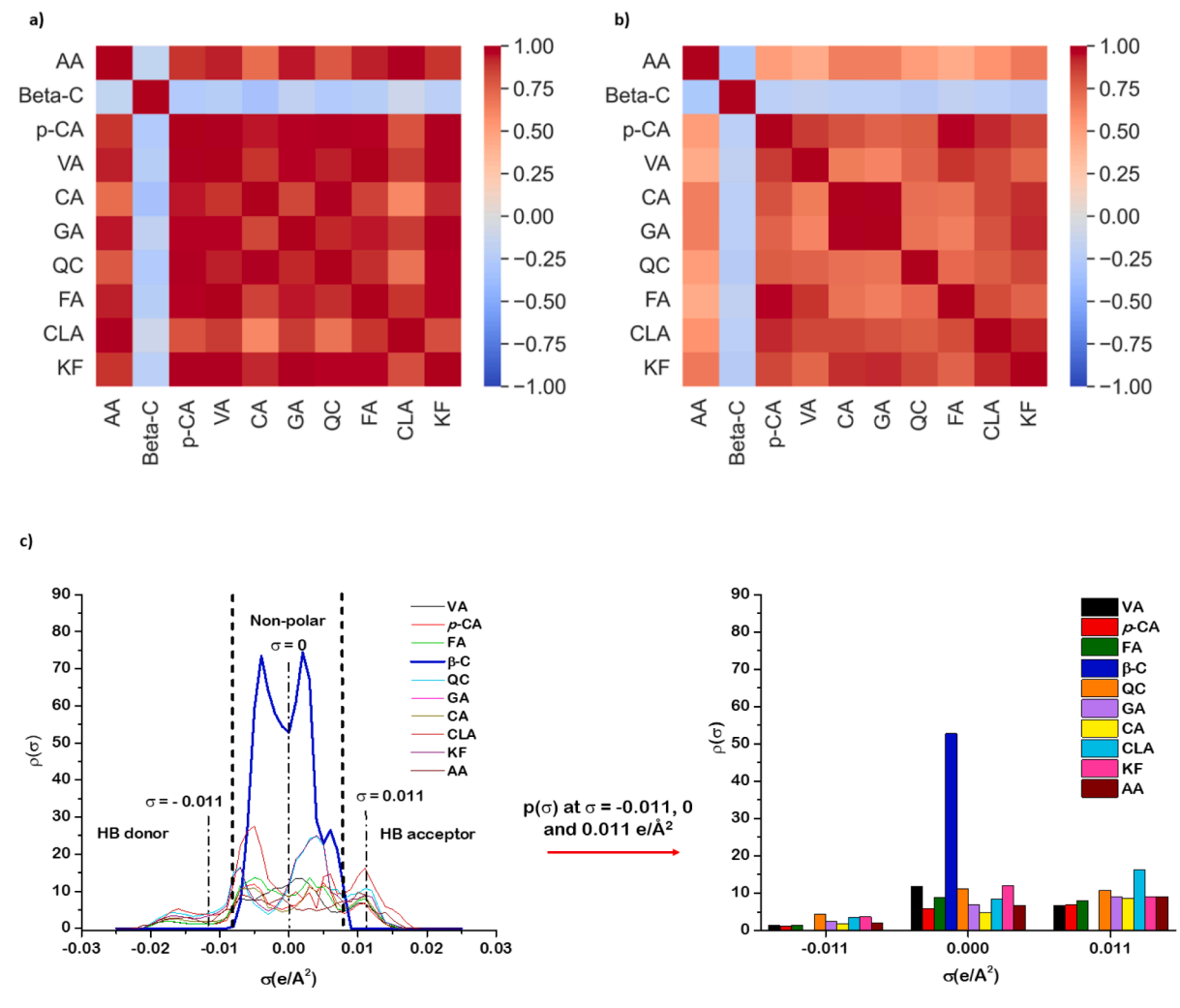


Fig. 2. A) correlation heat map of the solubility of 10 FW extractives. Solubility data is obtained from COSMO-RS (ADF-SCM) for each solute in 2400 + solvents. b) Correlation heat map of the HSPiP predicted distance between 10 FW extractives and 2400 + solvents. c) COSMO-RS generated σ-profiles and surface charge densities of all FW extractives at σ (e/Å²) = -0.011, 0, and 0.011. VA, *p*-CA, FA, β-C or beta-C, QC, GA, CA, CLA, KF, and AA stand for vanillic acid, *p*-coumaric acid, ferulic acid, β-carotene, quercetin, gallic acid, caffeic acid, chlorogenic acid, kaempferol, and ascorbic acid, respectively.

solvents (cyclohexanone, methyl isobutyl ketone, 2-propanol, ethanol, 2-pentanone, 2,4,6-trimethylpyridine, dimethyl sulfoxide (DMSO), dimethylformamide (DMF), and cyclohexanol) that possess the highest solubility (COSMO-RS) for the extractives (except for carotene) and are green/yellow.

These selected green/yellow solvents were evaluated for five solutes (p-coumaric acid, ferulic acid, vanillic acid, quercetin, and β -carotene) to assess the accuracy of the COSMO-RS. The parity plot of experimental vs. predicted solubility (Fig. 3) provides three significant results: a) DMF exhibits the highest solubility for quercetin, p-coumaric, ferulic, and vanillic acid, while cyclohexanol provides the highest solubility for β -carotene; b) COSMO-RS is qualitatively correct, and c) COSMO-RS overpredicts the solubility of β -carotene in 7 out of 9 solvents (except for cyclohexanol and DMSO) and in 8 out of 9 solvents (excluding DMF) for the rest. Therefore, COSMO-RS is excellent for the rapid identification of high-performance solvents. However, it lacks quantitative agreement, consistent with the literature (see methods) [64,65].

FDA Q3C Guidance for Industry (2003) lists DMF as a Class 2 solvent (yellow solvent) and recommends limited use (8.8 mg/day). Using these extractives in the pharmaceutical, cosmetic, and food industries necessitates green solvents [57]. Thus, the substitution of DMF for green solvent(s) can be impactful. We evaluated high-performing greener substitutes for DMF, using HSPiP on the CHEM21 recommended green

solvent list [58] and the list of identified 58 green and yellow solvents (except DMF) with quercetin as a test case (as 9 out of 10 solutes except β-carotene are positively correlated). HSPiP finds a better mixture in Chem21 with a smaller distance from DMF (0.4). 74% DMSO and 26% tert-butyl alcohol (Mixture 1) is predicted as the best replacement for DMF and 61% cyclohexanone and 39% ethylene glycol (Mixture 2) as the best mixture for solubilizing quercetin (Supplementary Table 7). The experimentally determined Hansen Solubility parameters and predicted distance have about \pm 0.5 (MPA)^{0.5} and \pm 1 (MPA)^{0.5} error, respectively [66]. HSPiP indicates the distance of quercetin from the solvent mixtures 1 and 2 as 7.8 and 7.1, respectively, which lies within this uncertainty range. Thus, the difference between the predicted distance is not significant enough to prefer one mixture over the other. Experimentally, Mixture 1 provides higher solubility (1.31 \pm 0.08 g/ml) than Mixture 2 (0.22 \pm 0.05 g/ml). COSMO-RS calculations independently confirmed this finding: the predicted solubilities are 2.016 g/ml and 0.563 g/ml, respectively. Mixture 1 provides the highest solubility for quercetin of all the tested green and yellow solvents except DMF (5.48 g/ ml). Experimental data for various compositions of Mixture 1 (Fig. 4) are consistent with the predicted ones and relatively flat around the optimum. We recommend that the composition is chosen by (a) optimizing experimentally around the HSPiP value and (b) considering the solvent cost. Our results demonstrate that a binary mixture of green solvents can

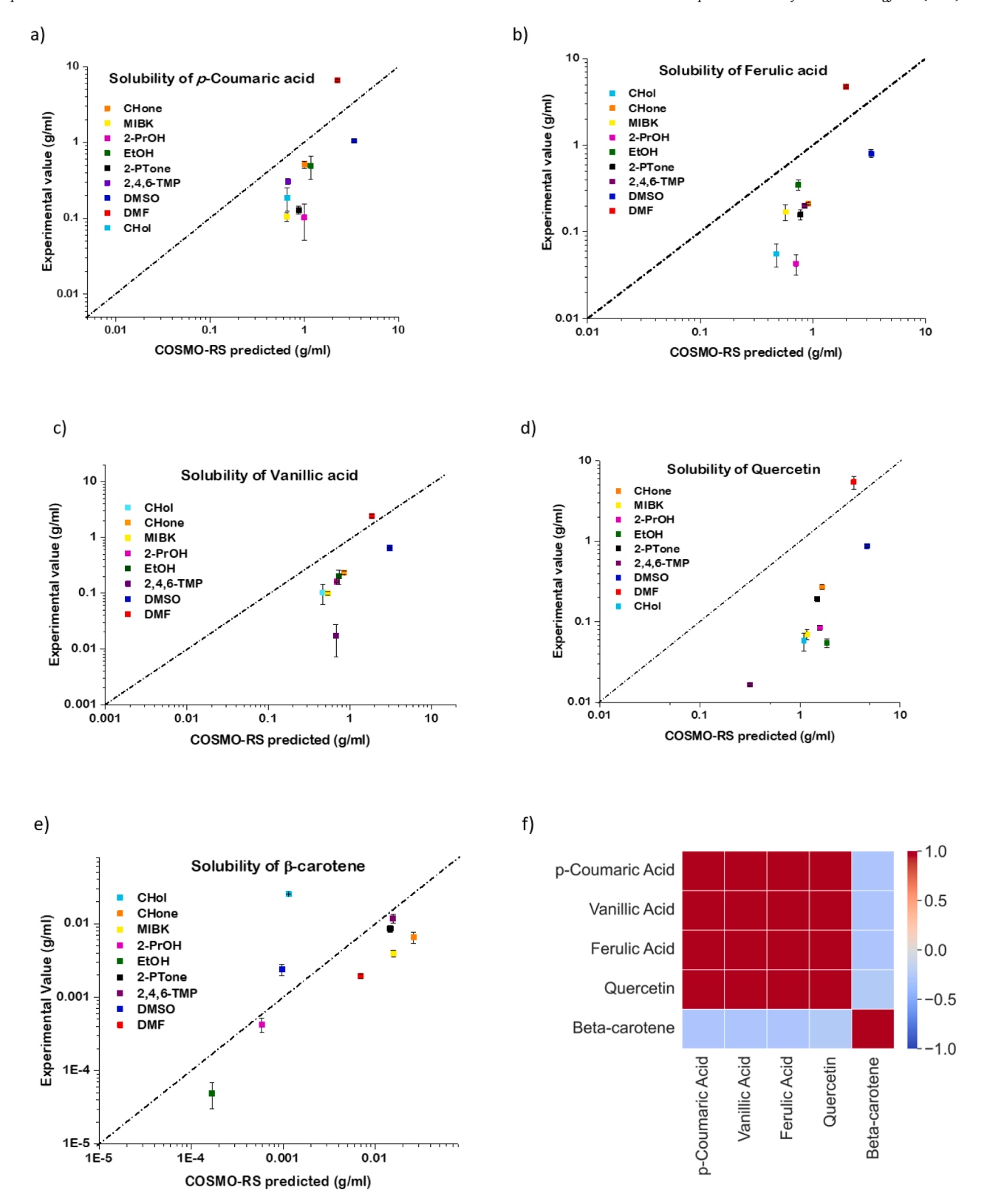


Fig. 3. Experimental vs. predicted solubility in 9 solvents for a) *p*-coumaric acid, b) ferulic acid, c) vanillic acid, d) quercetin, and e) β-carotene. f) Correlation heat map of experimental solubility of 5 FW extractives. EtOH, 2-PrOH, CHol, CHone, DMF, DMSO, MIBK, 2,4,6-TMP, and 2-Prone stand for ethanol, 2-propanol, cyclohexanol, cyclohexanone, dimethyl formamide, dimethyl sulfoxide, methyl isobutyl ketone, 2,4,6-trimethylpyridine, and 2-pentanone, respectively.

replace a single non-green solvent but is not superior to DMF in terms of extraction efficiency. Yet, identifying a high-performing solvent, such as DMF, defines a target for green solvent mixtures that are similar in performance. Given the limited size of the Chem21 database, there is an

opportunity to find better solvent mixtures by expanding the list to replace DMF.

Next, we turn to provide insights into solvent selection. Given that the nine compounds are suitable HB donors, good HB acceptor solvents

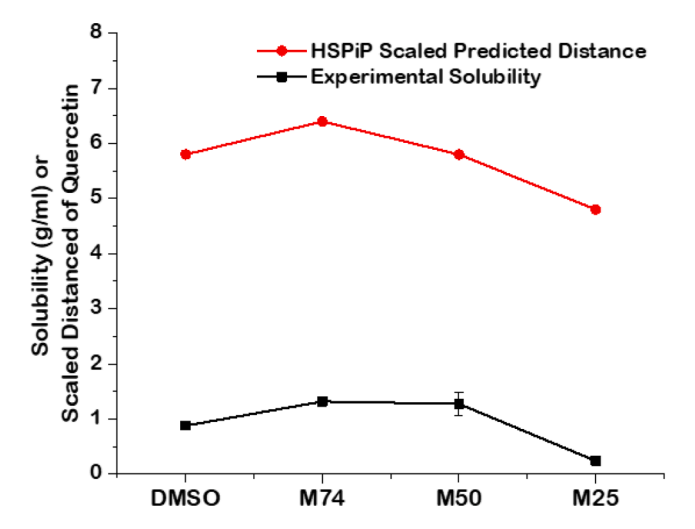


Fig. 4. Experimentally observed and HSPiP predicted solubilities for green solvents mixtures. M74, M50, and M25 are mixtures of DMSO with 26%, 50%, and 75% *tert*-butylalcohol, respectively. HSPiP scaled distance = (1/predicted distance) *50. HSPiP distance is scaled for demonstration purposes only. (For interpretation of the references to colour in this figure legend, the reader is referred to the web version of this article.)

perform better. Stemming from the statement 'like dissolves like,' polar solvents are expected to be better due to stronger dipole-dipole interactions. Experimentally, DMF and DMSO are the best for all four solutes. HSPiP indicates that DMSO has a high δP (Supplementary Table 7) while DMF has a higher δH. DMF with a molecular formula of (CH₃)₂NC(O)H comprises two electronegative atoms, N and O, making it a stronger HB acceptor than DMSO ((CH₃)₂SO). The σ -profiles (Fig. 5a) show that DMF and DMSO have low non-polar surface charge density (p $(\sigma(e/Å^2) = 0)$) and high HB acceptor surface charge densities $(\sigma(e/Å^2) >$ 0.0079). Their lower HB donor region ($\sigma(e/\mathring{A}^2) < -0.0079$) does not affect performance. COSMO-RS predicts DMSO to have a higher solubility than DMF in contrast to experimental results, and HSPiP caused due to underlying model assumptions discussed above. Our work indicates that these computational tools have limited accuracy and could be applied as screening tools to identify top solvents. Experiments are essential for validation.

The σ -profiles (Fig. 5b) reveal subtle differences between DMF and Mixtures 1 and 2, consistent with the HSPiP predictions. Mixture 1 has a lower non-polar peak (at (σ (e/Ų) = 0) and a higher HB acceptor surface change density than Mixture 2 and provides higher solubility than Mixture 2 but lower than DMF, as also experimentally observed. Thus, polarity and HB are key solvent parameters for extracting polar and acidic extractives. For β -carotene ($\delta P = 0.83$; $\delta H = 1.9$), non-polar solvents (such as MIBK, cyclohexanone, 2,4,6-trimethylpyridine) perform

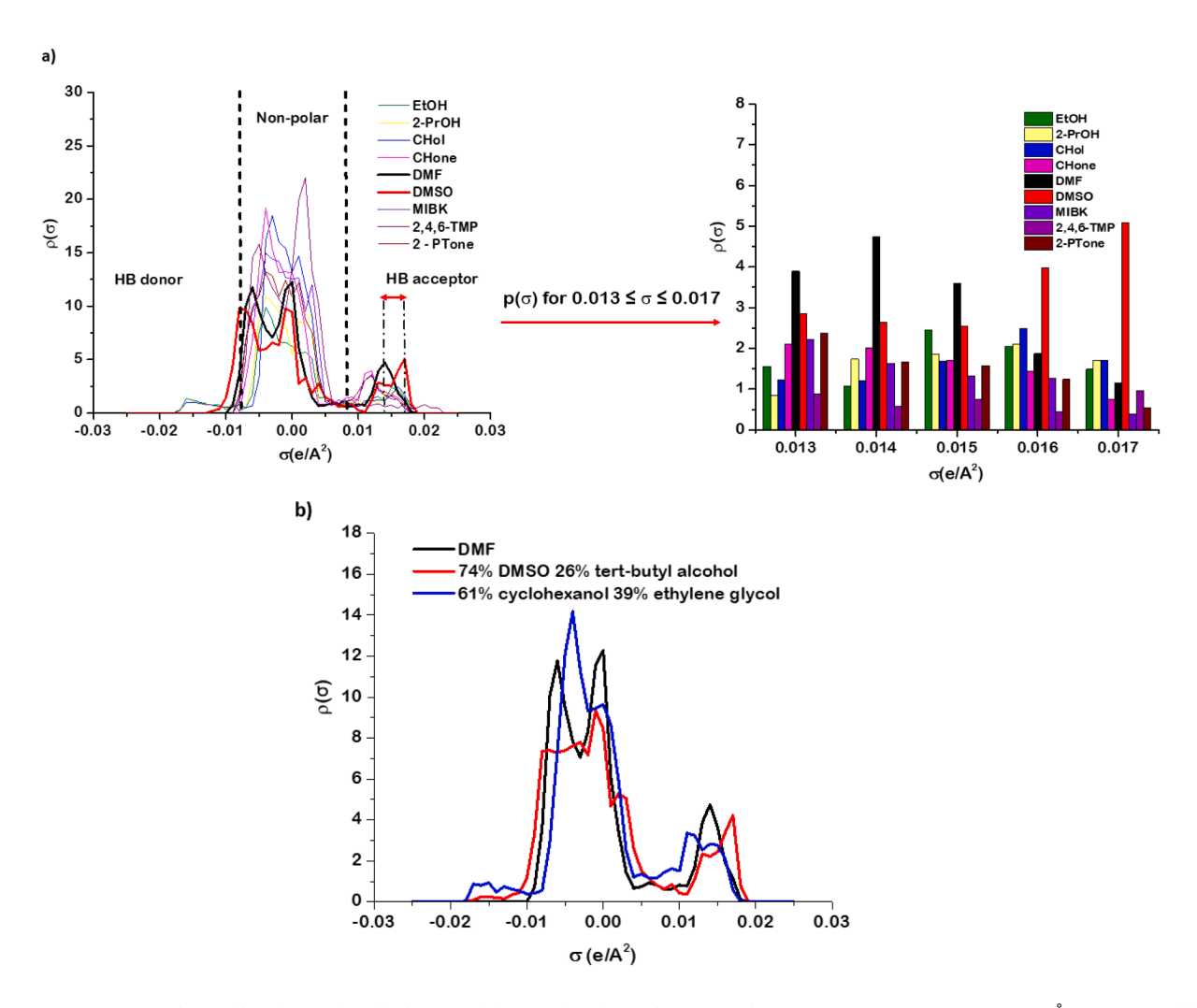


Fig. 5. COSMO-RS generated σ -profiles of a) 9 selected solvents and their surface charge densities in the HB acceptor region at $0.013 \le \sigma$ (e/Å2) ≤ 0.017 and b) DMF and green solvent mixtures. EtOH, 2-PrOH, CHol, CHone, DMF, DMSO, MIBK, 2,4,6-TMP, and 2-PTone stand for ethanol, 2-propanol, cyclohexanol, cyclohexanone, dimethyl formamide, dimethyl sulfoxide, methyl isobutyl ketone, 2,4,6-trimethylpyridine, and 2-pentanone, respectively. (For interpretation of the references to colour in this figure legend, the reader is referred to the web version of this article.)

Table 3Total phenolic content (TPC) and weight percent extracted from PPW in different solvents using Soxhlet and concentration of acids extracted in a one pot from PPW in different solvents.

Solvent	TPC (mg GAE/ g) [†]	Weight percent extracted (%) [†]	Caffeic acid (µg/ ml) ◆	Chlorogenic acid (µg/ml)❖	p-Coumaric acid (μg/ ml)❖
DMF	3.86	19	0.89 ±	0.26 ± 0.03	0.32 ± 0.07
	± 0.22		0.06		
Ethanol	1.55	4.03	$0.60 \pm$	ND*	0.12 ± 0.01
	± 0.13		0.01		
Methanol	3.89	2.11	$0.99~\pm$	1.36 ± 0.23	0.16 ± 0.06
	± 0.19		0.07		
Water	7.28	15	$0.25~\pm$	ND*	0.05 ± 0.03
	± 0.16		0.01		
Mixture	1.17	8.2	0.46 \pm	0.76 ± 0.05	0.11 ± 0.08
1	$\pm~0.03$		0.04		

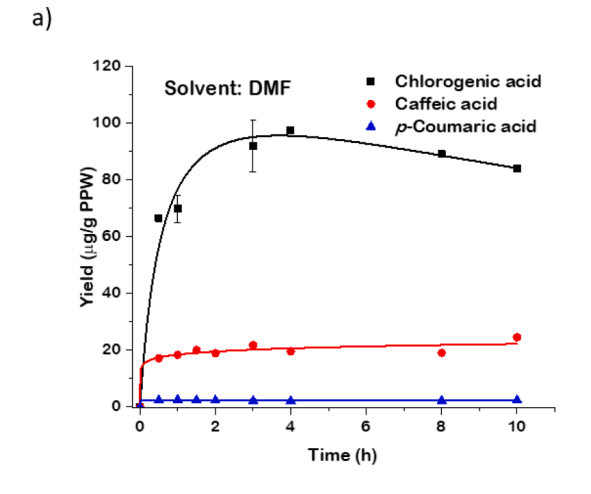
^{*} ND: Not detected.

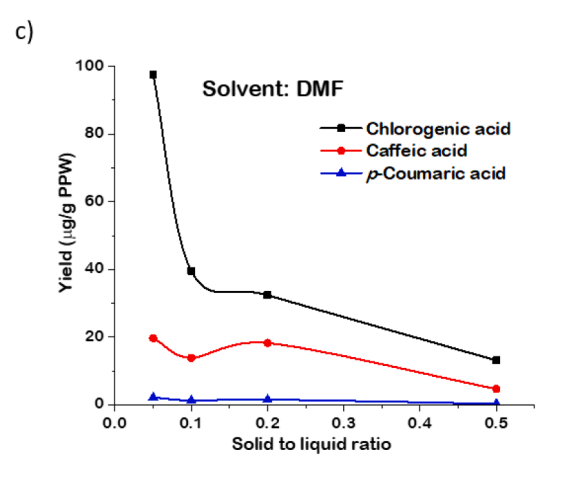
better and HB is not an essential factor.

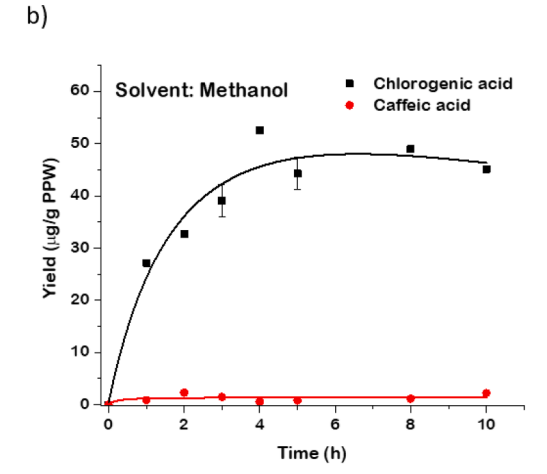
3.3. Application to potato peel waste (PPW)

Potato peel waste (PPW) is rich in various phenolics, e.g., chlorogenic acid, caffeic acid, p-coumaric acid, and ferulic acid [16]. Our work above indicated that DMF provides the highest solubility for these compounds. The moisture content in dry PPW (3.54%) does not hinder the solubilization of the target compounds, as the HSPiP predicted distance of the mixture of DMF and water only changes by 0.34 ± 0.10 in comparison to pure DMF for all extractives (Supplementary Table 8). For the phenolic acids and flavonoids, the distance decreased, while for β -carotene increased. The observed difference is due to the change of the HB parameter that changes with the addition of water.

In Soxhlet extraction, the FW matrix is not directly exposed to heat, and extraction is conducted until the solvent appears colorless in the thimble. In contrast, the extractives dissolved in a solvent are heated for long time and can be degraded. Thus, Soxhlet can provide the maximum theoretical extraction (weight percent) from FW [27]. To assess the concentration of acids extracted from PPW, we conducted one-pot extraction from PPW in DMF, Mixture 1, and three commonly used solvents, namely ethanol, methanol, and water. Table 3 shows that DMF is superior in the total weight percent extracted from PPW, followed by water. The ability of water to dissolve other components, such as carbohydrates [68] in FW assists obtaining a high weight percent. Mixture 1 is better than methanol and ethanol but inferior to DMF and water. Additionally, Table 3 shows that the extraction of target acids from PPW







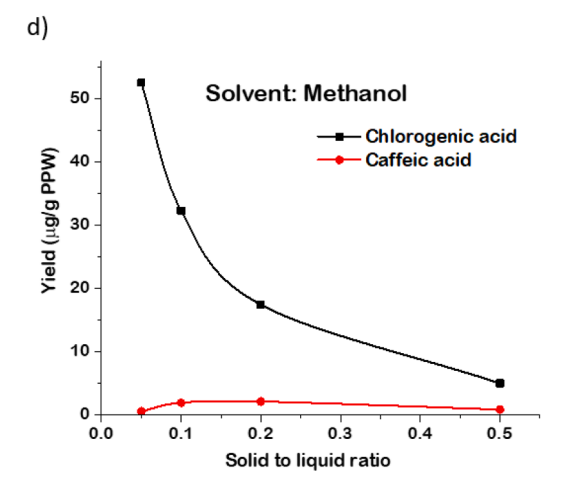


Fig. 6. Time-dependent extractions from PPW using a) DMF and b) methanol at 60 °C and 1:20 solid-to-liquid ratio. Extraction from PPW at different solid-to-liquid ratios using c) DMF and d) methanol at 60 °C and 4 h. The solid lines are for visual interpretation only.

 $^{^\}dagger$ Total phenolic content (TPC) and weight percent extracted from PPW in different solvents using Soxhlet.

Concentration of acids extracted in a one pot from PPW in different solvents.

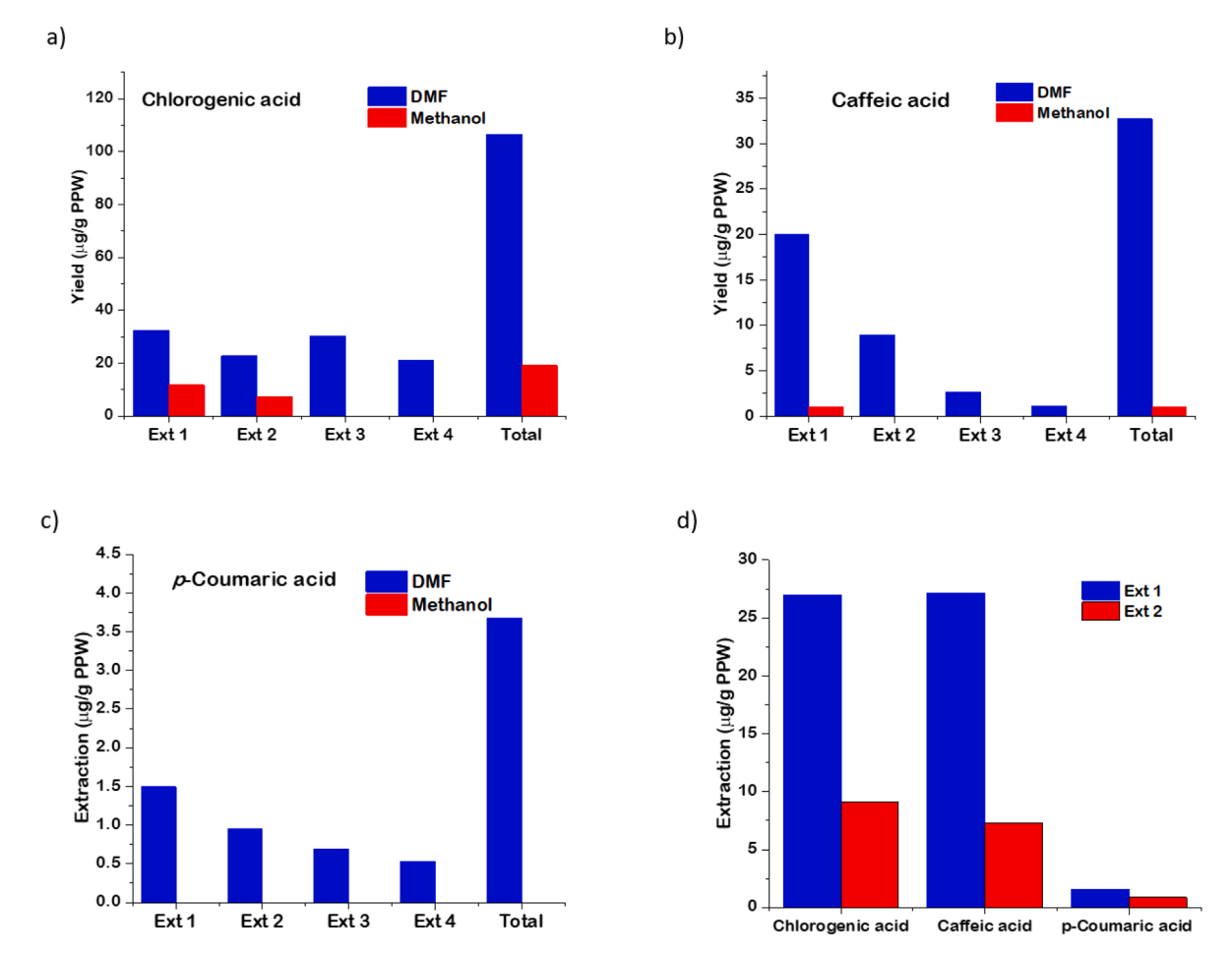


Fig. 7. Yield of a) chlorogenic, b) caffeic, and c) *p*-coumaric acid in four extraction cycles using fresh solvent and recycled PPW in every cycle using DMF and methanol. d) Yield of chlorogenic, caffeic, and *p*-coumaric acids over two cycles using fresh PPW and recycled DMF for a second cycle. Ext denotes extraction.

in water is lower than in DMF.

It has been reported that the antioxidant capacity of the phenolic compounds is strongly reduced when they form HBs with the solvent. The total phenolic content (TPC) test was quantified using the traditional Folin-Ciocalteau reagent, i.e., the gallic acid equivalence method (GAE); see methods. This reagent measures the overall reducing capacity of the sample in addition to the phenolic compounds. The data is summarized in Table 3. Water provides the highest TPC followed by DMF and methanol, and finally ethanol. DMF and Mixture 1 have a relatively low TPC despite high extraction ability due to HB with the compounds.

According to the one-pot extraction from PPW, methanol provides a higher concentration of caffeic and chlorogenic acid. However, the extraction of acids is expected to increase when the temperature is above $60\,^{\circ}\text{C}$. Unlike methanol, limited by its boiling point, there is potential for optimizing the temperature in DMF and Mixture 1 to increase extraction efficiency even further. We established a protocol to compare the results between methanol and DMF. The time needed for equilibration was estimated (Fig. 6a and 6b). The chlorogenic acid yield increases until 4 h and then either stays constant or decreases slightly at longer times (~10% change). The phenolic acids can interact with other extracted FW components, such as starch, by supramolecular complexation and undergo enzymatic reactions with polyphenol oxidase and glycolytic enzymes. The observed decline at longer times (Supplementary Fig. 1) can then be attributed to such enzymatic reactions, given that chlorogenic acid is thermally stable at low temperatures [69-71]. Following this, the extraction with respect to the solid-to-liquid (S:L) ratio was also studied (Fig. 6c and 6d) at 60 °C. Both solvents provide the highest yield of chlorogenic acid at 4 h, while caffeic and p-coumaric acid yields do

not change significantly over time. Further, a steep decline in the yield of chlorogenic acid can be seen in DMF and methanol as the S:L ratio is increased from 0.05 to 0.1. Solid wetting issues, such as PPW sticking to the wall, can hinder efficient extraction at high S:L ratios. The yield of caffeic and *p*-coumaric acid in DMF decreases steadily and does not change much at high S:L ratios. DMF extracts at least 1.8 times more chlorogenic acid than methanol at every S:L ratio.

The re-extraction efficiency is essential to recover all target products. We reused the solvent over two cycles to explore if it could be reused. A decline in the yield was seen (Fig. 7d). As discussed above, the enzymatic reactions occurring in the multi-component system possibly cause the observed reduction in the yield of extracted compounds. Thus, separating target acids after each extraction is essential and strongly recommended.

Next, extraction cycles were conducted in methanol and DMF at 60 °C and 1:5 S:L ratio for 4 h reusing PPW and fresh solvent in each cycle (Fig. 7a-c). The chlorogenic (106.6 $\mu g/g$ PPW) and caffeic acid (32.7 $\mu g/g$ PPW) yield in DMF after four extractions is ~ 5 and ~ 32 times higher than in methanol, respectively. DMF achieves nearly equal extraction of chlorogenic acid in each cycle, while methanol provides no yield after two cycles. Methanol provides very low yields of p-coumaric acid (<0.02 $\mu g/g$ PPW), while DMF gives a total 3.67 $\mu g/g$ PPW in four cycles. Increased interaction of polar aprotic DMF with cellulose, hemicellulose and lignin in the cell walls helps the permeation and disruption, releasing higher amounts of phenolic acids. The data indicates that it is worth performing a few extraction cycles for the same waste stream and that DMF is more efficient than traditional solvents. The higher efficiency of DMF could lead to an overall reduction in the cost of the solvent and effective feedstock utilization. The superiority of

DMF over traditional solvents can also be confirmed with other types and mixtures of food wastes enriched in the target phenolic compounds.

4. Conclusions

We identified the ten most commonly found antimicrobial activity possessing phenols and antioxidant flavonoids in different FW feedstocks. We have used COSMO-RS and HSPiP computations for rapid screening and insights and considered lists of green and yellow solvents. We found 9 out of the 10 target compounds are strongly correlated, and thus, solubility findings transfer among them (excluding β-carotene); this minimizes the experimental work. Experimental data using selected green/yellow solvents affirm the predictions of COSMO-RS and HSPiP. DMF and DMSO are the top single solvents for the target compounds; the former is superior (15x) to the commonly used methanol and ethanol. Since DMF's use is limited, green solvent mixtures (74% DMSO and 26% tert-butyl alcohol and 61% cyclohexanone and 39% ethylene glycol) with high solubility were predicted and tested experimentally. Experimental validation is crucial as the computational tools have limited accuracy. We then translated these pure compound solubility results to actual potato peel waste. The approach can be extended to other solutes and feedstocks to design extraction processes for a circular economy.

CRediT authorship contribution statement

Yagya Gupta: Conceptualization, Methodology, Writing – original draft. Souryadeep Bhattacharyya: Methodology. Dionisios G. Vlachos: Conceptualization, Methodology, Writing – review & editing.

Declaration of Competing Interest

The authors declare that they have no known competing financial interests or personal relationships that could have appeared to influence the work reported in this paper.

Data availability

The authors have shared data used for this research in the supplementary information.

Acknowledgments

This work was intellectually driven and supported as part of the Catalysis Center for Energy Innovation, an Energy Frontier Research Center funded by the US Dept. of Energy, Office of Science, Office of Basic Energy Sciences under award number DE-SC0001004. The later stages of this work were supported by the National Science Foundation (NSF GCR CMMI 1934887). Y.G. wants to thank Dr. S. Sadula for supervision at the project initiation and E. Ebikade for the discussions during the project. The authors acknowledge the Advanced Material Characterization Laboratory (AMCL) at the University of Delaware.

Appendix A. Supplementary material

Supplementary data to this article can be found online at $\frac{https:}{doi.}$ org/10.1016/j.seppur.2023.123719.

References

- M. Blakeney, Food loss and food waste: Causes and solutions, Edward Elgar Publishing (2019), https://doi.org/10.4337/9781788975391.
- [2] FAO IFAD UNICEF WFP and WHO, The State of Food Security and Nutrition in the World, 2019. Safeguarding against economic slowdowns and downturns, Rome, FAO. License: CC BY-NC-SA 3.0 IGO, 2019. 10.26596/wn.201910395-97.
- [3] Y. Li, Y. Chen, J. Wu, Enhancement of methane production in anaerobic digestion process: A review, Appl. Energy 240 (2019) 120–137, https://doi.org/10.1016/j. apenergy.2019.01.243.

- [4] M. Crippa, E. Solazzo, D. Guizzardi, F. Monforti-Ferrario, F.N. Tubiello, A. Leip, Food systems are responsible for a third of global anthropogenic GHG emissions, Nat Food. 2 (2021) 198–209, https://doi.org/10.1038/s43016-021-00225-9.
- [5] F. Xu, Y. Li, X. Ge, L. Yang, Y. Li, Anaerobic digestion of food waste Challenges and opportunities, Bioresour. Technol. 247 (2018) 1047–1058, https://doi.org/ 10.1016/j.biortech.2017.09.020.
- [6] Z. Li, H. Lu, L. Ren, L. He, Experimental and modeling approaches for food waste composting: A review, Chemosphere 93 (2013) 1247–1257, https://doi.org/ 10.1016/j.chemosphere.2013.06.064.
- [7] C. Nathao, U. Sirisukpoka, N. Pisutpaisal, Production of hydrogen and methane by one and two stage fermentation of food waste, Int. J. Hydrogen Energy 38 (2013) 15764–15769, https://doi.org/10.1016/j.ijhydene.2013.05.047.
- [8] Formal Agreement Among EPA, FDA, and USDA Relative to Cooperation and Coordination on Food Loss and Waste, U.S. Food and Drug Administration. (2020). https://www.fda.gov/food/domestic-interagency-agreements-food/formal-agree ment-among-epa-fda-and-usda-relative-cooperation-and-coordination-food-loss-a nd-waste (accessed October 31, 2022).
- [9] T. Voituriez, K. Morita, T. Giordano, N. Bakkour, N. Shimizu, Financing the 2030 agenda for sustainable development, Governing Through Goals: Sustainable Development Goals as Governance, Innovation. 16301 (2017) 259–273, https://doi.org/10.7551/mitpress/9780262035620.003.0011.
- [10] M.J. Lindsay, T.W. Walker, J.A. Dumesic, S.A. Rankin, G.W. Huber, Production of monosaccharides and whey protein from acid whey waste streams in the dairy industry, Green Chem. 20 (2018) 1824–1834, https://doi.org/10.1039/ csep05176
- [12] L. Cao, I.K.M. Yu, D.C.W. Tsang, S. Zhang, Y.S. Ok, E.E. Kwon, H. Song, C.S. Poon, Phosphoric acid-activated wood biochar for catalytic conversion of starch-rich food waste into glucose and 5-hydroxymethylfurfural, Bioresour. Technol. 267 (2018) 242–248, https://doi.org/10.1016/j.biortech.2018.07.048.
- [13] T.P.T. Pham, R. Kaushik, G.K. Parshetti, R. Mahmood, R. Balasubramanian, Food waste-to-energy conversion technologies: Current status and future directions, Waste Manag. 38 (2015) 399–408, https://doi.org/10.1016/j.wasman.2014.12.004.
- [14] E.O. Ebikade, S. Sadula, Y. Gupta, D.G. Vlachos, A review of thermal and thermocatalytic valorization of food waste, Green Chemistry. (2021) 2806–2833. 10.1039/d1gc00536g.
- [15] M.L. Stone, E.M. Anderson, K.M. Meek, M. Reed, R. Katahira, F. Chen, R.A. Dixon, G.T. Beckham, Y. Román-Leshkov, Reductive Catalytic Fractionation of C-Lignin, ACS Sustain. Chem. Eng. 6 (2018) 11211–11218, https://doi.org/10.1021/ acssuschemeng.8b02741.
- [16] E. Ebikade, A. Athaley, B. Fisher, K. Yang, C. Wu, M.G. Ierapetritou, D.G. Vlachos, The Future is Garbage: Repurposing of Food Waste to an Integrated Biorefinery, ACS Sustain. Chem. Eng. 8 (2020) 8124–8136, https://doi.org/10.1021/ acssuschemeng.9b07479.
- [17] R. Kale, R. Deshmukh, Antioxidants Market by Type: Global Opportunity Analysis and Industry Forecast, 2022-2031, Allied Market Research. (2022). https://www. alliedmarketresearch.com/anti-oxidants-market (accessed October 31. 2022).
- [18] R. González-Montelongo, M. Gloria Lobo, M. González, Antioxidant activity in banana peel extracts: Testing extraction conditions and related bioactive compounds, Food Chem. 119 (2010) 1030–1039, https://doi.org/10.1016/j. foodchem.2009.08.012.
- [19] X.L. Bai, T.L. Yue, Y.H. Yuan, H.W. Zhang, Optimization of microwave-assisted extraction of polyphenols from apple pomace using response surface methodology and HPLC analysis, J. Sep. Sci. 33 (2010) 3751–3758, https://doi.org/10.1002/ jssc.201000430.
- [20] H. Li, Z. Deng, T. Wu, R. Liu, S. Loewen, R. Tsao, Microwave-assisted extraction of phenolics with maximal antioxidant activities in tomatoes, Food Chem. 130 (2012) 928–936. https://doi.org/10.1016/j.foodchem.2011.08.019.
- [21] B.B. Li, B. Smith, M.M. Hossain, Extraction of phenolics from citrus peels: I, Solvent extraction method, Sep Purif Technol. 48 (2006) 182–188, https://doi.org/ 10.1016/j.seppur.2005.07.005.
- [22] K. Krishnaswamy, V. Orsat, Y. Gariépy, K. Thangavel, Optimization of Microwave-Assisted Extraction of Phenolic Antioxidants from Grape Seeds (Vitis vinifera), Food Bioproc. Tech. 6 (2013) 441–455, https://doi.org/10.1007/s11947-012-0800-2
- [23] X. Xiong, I.K.M. Yu, D.C.W. Tsang, N.S. Bolan, Y. Sik Ok, A.D. Igalavithana, M. B. Kirkham, K.H. Kim, K. Vikrant, Value-added chemicals from food supply chain wastes: State-of-the-art review and future prospects, Chem. Eng. J. 375 (2019), https://doi.org/10.1016/j.cej.2019.121983.
- [24] Z. Wang, S. Bhattacharyya, D.G. Vlachos, Extraction of Furfural and Furfural/5-Hydroxymethylfurfural from Mixed Lignocellulosic Biomass-Derived Feedstocks, ACS Sustain. Chem. Eng. 9 (2021) 7489–7498, https://doi.org/10.1021/ acssuschemeng.1c00982.
- [25] Z. Wang, S. Bhattacharyya, D.G. Vlachos, Solvent selection for biphasic extraction of 5-hydroxymethylfurfural: Via multiscale modeling and experiments, Green Chem. 22 (2020) 8699–8712, https://doi.org/10.1039/d0gc03251d.
- [26] Environmental Protection Agency. United States, Product Properties Test Guidelines. OPPTS 830.7840. Water Solubility: Column Elution Method; Shake Flask Method (EPA 712-C-98-041), 1998. https://nepis.epa.gov/Exe/ZyPURL.cgi? Dockey=P1005E0Q.txt (accessed October 31, 2022).
- [27] B. Hames, R. Ruiz, C. Scarlata, A. Sluiter, J. Sluiter, D. Templeton, Preparation of Samples for Compositional Analysis: Laboratory Analytical Procedure (LAP); NREL/TP-510-42620, National Renewable Energy Laboratory. (2008).
- [28] A. Ismail, Z.M. Marjan, C.W. Foong, Total antioxidant activity and phenolic content in selected vegetables, Food Chem. 87 (2004) 581–586, https://doi.org/10.1016/j. foodchem.2004.01.010.

- [29] A. Fredenslund, R.L. Jones, J.M. Prausnitz, Group-contribution estimation of activity coefficients in nonideal liquid mixtures, AIChE J 21 (1975) 1086–1099, https://doi.org/10.1002/aic.690210607.
- [30] J. Gmehling, J. Li, M. Schiller, A Modified UNIFAC Model. 2. Present Parameter Matrix and Results for Different Thermodynamic Properties, Ind. Eng. Chem. Res. 32 (1993) 178–193, https://doi.org/10.1021/ie00013a024.
- [31] E. Mullins, Y.A. Liu, A. Ghaderi, S.D. Fast, Sigma profile database for predicting solid solubility in pure and mixed solvent mixtures for organic pharmacological compounds with COSMO-based thermodynamic methods, Ind. Eng. Chem. Res. 47 (2008) 1707–1725, https://doi.org/10.1021/ie0711022.
- [32] AMS 2019.3 COSMO-RS, SCM. (2019). http://www.scm.com (accessed May 9, 2020)
- [33] C.C. Pye, T. Ziegler, An implementation of the conductor-like screening model of solvation within the Amsterdam density functional package, Theor. Chem. Acc. 101 (1999) 396–408, https://doi.org/10.1007/s002140050457.
- [34] A.M. Booth, T. Bannan, M.R. McGillen, M.H. Barley, D.O. Topping, G. McFiggans, C.J. Percival, The role of ortho, meta, para isomerism in measured solid state and derived sub-cooled liquid vapour pressures of substituted benzoic acids, RSC Adv. 2 (2012) 4430–4443, https://doi.org/10.1039/c2ra01004f.
- [35] A. Noubigh, M. Abderrabba, Solid-liquid phase equilibrium and thermodynamic properties of vanillic acid in different pure solvents, J. Mol. Liq. 223 (2016) 261–266, https://doi.org/10.1016/j.molliq.2016.07.004.
- [36] M.S. Manic, D. Villanueva, T. Fornari, A.J. Queimada, E.A. MacEdo, V. Najdanovic-Visak, Solubility of high-value compounds in ethyl lactate: Measurements and modeling, J. Chem. Thermodyn. 48 (2012) 93–100, https://doi.org/10.1016/j. ict.2011.12.005
- [37] S.M. Vilas-Boas, V. Vieira, P. Brandão, R.S. Alves, J.A.P. Coutinho, S.P. Pinho, O. Ferreira, Solvent and temperature effects on the solubility of syringic, vanillic or veratric acids: Experimental, modeling and solid phase studies, J. Mol. Liq. 289 (2019), https://doi.org/10.1016/j.molliq.2019.111089.
- [38] Y. Zhang, F. Guo, Q. Cui, M. Lu, X. Song, H. Tang, Q. Li, Measurement and Correlation of the Solubility of Vanillic Acid in Eight Pure and Water + Ethanol Mixed Solvents at Temperatures from (293.15 to 323.15) K, J. Chem. Eng. Data 61 (2016) 420–429, https://doi.org/10.1021/acs.jced.5b00619.
- [39] K.A. Park, H.J. Lee, I.K. Hong, Solubility prediction of bioantioxidants for functional solvent by group contribution method, J. Ind. Eng. Chem. 16 (2010) 490–495, https://doi.org/10.1016/j.jiec.2010.01.060.
- [40] Y. Corvis, M.C. Menet, P. Négrier, M. Lazerges, P. Espeau, The role of stearic acid in ascorbic acid protection from degradation: A heterogeneous system for homogeneous thermodynamic data, New J. Chem. 37 (2013) 761–768, https://doi. org/10.1039/e7ji40933i
- [41] C.S. Su, Y.M. Chen, Y.P. Chen, Correlation of solid solubilities for phenolic compounds and steroids in supercritical carbon dioxide using the solution model, J. Taiwan Inst. Chem. Eng. 42 (2011) 608–615, https://doi.org/10.1016/j. iiice 2010 11 005
- [42] F.L. Mota, A.J. Queimada, S.P. Pinho, E.A. Macedo, Aqueous solubility of some natural phenolic compounds, Ind. Eng. Chem. Res. 47 (2008) 5182–5189, https:// doi.org/10.1021/je0714520
- [43] C.S. Su, Y.P. Chen, Correlation for the solubilities of pharmaceutical compounds in supercritical carbon dioxide, Fluid Phase Equilib. 254 (2007) 167–173, https://doi. org/10.1016/j.fluid.2007.03.004.
- [44] E.I. Alevizou, E.C. Voutsas, Solubilities of p-coumaric and caffeic acid in ionic liquids and organic solvents, J. Chem. Thermodyn. 62 (2013) 69–78, https://doi. org/10.1016/j.ict.2013.02.013.
- [45] L. Chebil, C. Humeau, J. Anthony, F. Dehez, J.M. Engasser, M. Ghoul, Solubility of flavonoids in organic solvents, J. Chem. Eng. Data 52 (2007) 1552–1556, https://doi.org/10.1021/je7001094.
- [46] T. Treszczanowicz, T. Kasprzycka-Guttman, A.J. Treszczanowicz, Solubility of β-Carotene in Binary Solvents Formed by Some Hydrocarbons with Dibutyl Ether and 1,2-Dimethoxyethane, J. Chem. Eng. Data 48 (2003) 1517–1520, https://doi. org/10.1021/je030165y.
- [47] T.O. Dabir, V.G. Gaikar, S. Jayaraman, S. Mukherjee, Thermodynamic modeling studies of aqueous solubility of caffeine, gallic acid and their cocrystal in the temperature range of 303 K–363 K, Fluid Phase Equilib. 456 (2018) 65–76, https:// doi.org/10.1016/j.fluid.2017.09.021.
- [48] R. Bogel-Łukasik, L.M. Nobre Gonçalves, E. Bogel-Łukasik, Phase equilibrium phenomena in solutions involving tannins, flavonoids and ionic liquids, Green Chem. 12 (2010) 1947–1953, https://doi.org/10.1039/c0gc00308e.
- [49] S.M. Vilas-Boas, P. Brandão, M.A.R. Martins, L.P. Silva, T.B. Schreiner, L. Fernandes, O. Ferreira, S.P. Pinho, Solubility and solid phase studies of isomeric phenolic acids in pure solvents, J. Mol. Liq. 272 (2018) 1048–1057, https://doi. org/10.1016/j.molliq.2018.10.108.
- [50] Kaempferol, PubChem. (2004). https://pubchem.ncbi.nlm.nih.gov/compound/K aempferol (accessed March 21, 2023).
- [51] Chlorogenic Acid, PubChem. (2004). https://pubchem.ncbi.nlm.nih.gov/compound/Chlorogenic-Acid (accessed March 21, 2023).
- [52] A. Klamt, V. Jonas, T. Bürger, J.C.W. Lohrenz, Refinement and parametrization of COSMO-RS, J. Phys. Chem. A 102 (1998) 5074–5085, https://doi.org/10.1021/ ip980017s
- [53] J. Scheffczyk, L. Fleitmann, A. Schwarz, M. Lampe, A. Bardow, K. Leonhard, COSMO-CAMD: A framework for optimization-based computer-aided molecular design using COSMO-RS, Chem. Eng. Sci. 159 (2017) 84–92, https://doi.org/ 10.1016/j.ces.2016.05.038.
- [54] A. Klamt, COSMO-RS: From Quantum Chemistry to Fluid Phase Thermodynamics, Comput. Aided Chem. Eng. 43 (2018) 9, https://doi.org/10.1016/B978-0-444-64235-6.50003-6.

- [55] A. Klamt, F. Eckert, W. Arlt, COSMO-RS: An alternative to simulation for calculating thermodynamic properties of liquid mixtures, Annu. Rev. Chem. Biomol. Eng. 1 (2010) 101–122, https://doi.org/10.1146/annurev-chembioeng-073009-100903
- [56] S. Wang, J.M. Stubbs, J.I. Siepmann, S.I. Sandler, Effects of conformational distributions on sigma profiles in COSMO theories, J. Phys. Chem. A 109 (2005) 11285–11294, https://doi.org/10.1021/jp053859h.
- [57] U.S. Department of Health and Human Services, Food and Drug Administration, Center for Drug Evaluation and research, Center for Biologics Evaluation and Research, Q3C — Tables and List Guidance for Industry, 2017. https://www.fda.gov/media/71/737/download.
- [58] D. Prat, A. Wells, J. Hayler, H. Sneddon, C.R. McElroy, S. Abou-Shehada, P.J. Dunn, CHEM21 selection guide of classical- and less classical-solvents, Green Chem. 18 (2015) 288–296, https://doi.org/10.1039/c5gc01008j.
- [59] N.G. Anderson, Solvent Selection, Practical Process Research & Development. (2000) 81–111. 10.1016/b978-012059475-7/50007-7.
- [60] D. Prat, O. Pardigon, H.W. Flemming, S. Letestu, V. Ducandas, P. Isnard, E. Guntrum, T. Senac, S. Ruisseau, P. Cruciani, P. Hosek, Sanofi's Solvent Selection Guide: A Step Toward More Sustainable Processes, Org. Process Res. Dev. 17 (2013) 1517–1525, https://doi.org/10.1021/op4002565.
- [61] F.P. Byrne, S. Jin, G. Paggiola, T.H.M. Petchey, J.H. Clark, T.J. Farmer, A.J. Hunt, C. Robert McElroy, J. Sherwood, Tools and techniques for solvent selection: green solvent selection guides, Sustain. Chem. Processes 4 (2016) 1–24, https://doi.org/ 10.1186/s40508-016-0051-z.
- [62] C.M. Hansen, The Three Dimensional Solubility Parameter and Solvent Diffusion Coefficient. Their Importance in Surface Coating Formulation, J. Paint Technol. (1967) 104.
- [63] M. Díaz de los Ríos, E. Hernández Ramos, Determination of the Hansen solubility parameters and the Hansen sphere radius with the aid of the solver add-in of Microsoft Excel, SN Appl. Sci. 2 (2020) 1–7, https://doi.org/10.1007/s42452-020-2512-v.
- [64] B. Schröder, L.M.N.B.F. Santos, I.M. Marrucho, J.A.P. Coutinho, Prediction of aqueous solubilities of solid carboxylic acids with COSMO-RS, Fluid Phase Equilib. 289 (2010) 140–147, https://doi.org/10.1016/j.fluid.2009.11.018.
- [65] S.T. Lin, S.I. Sandler, A priori phase equilibrium prediction from a segment contribution solvation model, Ind. Eng. Chem. Res. 41 (2002) 899–913, https:// doi.org/10.1021/ie001047w.
- [66] R.J. Lehnert, R. Schilling, Accuracy of molar solubility prediction from hansen parameters. An exemplified treatment of the bioantioxidant l-ascorbic acid, Applied Sciences (Switzerland) 10 (2020), https://doi.org/10.3390/app10124266.
- [68] M. Borrega, K. Nieminen, H. Sixta, Degradation kinetics of the main carbohydrates in birch wood during hot water extraction in a batch reactor at elevated temperatures, Bioresour. Technol. 102 (2011) 10724–10732, https://doi.org/ 10.1016/j.bjortech.2011.09.027.
- [69] R.K. Sharma, T.S. Fisher, M.R. Hajaligol, Effect of reaction conditions on pyrolysis of chlorogenic acid, J. Anal. Appl. Pyrol. 62 (2002) 281–296, https://doi.org/ 10.1016/S0165-2370(01)00126-7.
- [70] D. Perrone, R. Donangelo, C.M. Donangelo, A. Farah, Modeling weight loss and chlorogenic acids content in coffee during roasting, J. Agric. Food Chem. 58 (2010) 12238–12243, https://doi.org/10.1021/jf102110u.
- [71] C.A.B. de Maria, L.C. Trugo, L.S. de Mariz, E. Miranda, E. Salvador, Stability of 5-caffeoylquinic acid under different conditions of heating, Food Research Internation. 31 (1998) 475–477.
- [72] L. Wartenberg, 10 Promising Benefits and Uses of Apple Pectin, Healthline. (2021). https://www.healthline.com/nutrition/apple-pectin.
- [73] M.A. Awad, A. de Jager, L.M. van Westing, Flavonoid and chlorogenic acid levels in apple fruit: characterisation of variation, Scientia, Horticulture 83 (2000) 249–263, https://doi.org/10.1016/S0304-4238(99)00124-7.
- [74] O.S. Omoba, R.O. Obafaye, S.O. Salawu, A.A. Boligon, M.L. Athayde, HPLC-DAD phenolic characterization and antioxidant activities of ripe and unripe sweet orange peels, Antioxidants. 4 (2015) 498–512, https://doi.org/10.3390/partice/40.20428
- [75] H.T. Vu, C.J. Scarlett, Q.V. Vuong, Phenolic compounds within banana peel and their potential uses: A review, J. Funct. Foods 40 (2018) 238–248, https://doi.org/ 10.1016/j.jff.2017.11.006.
- [76] M.J. Periago, I. Martínez-Valverde, A. Chesson, G. Provan, Phenolic compounds, lycopene and antioxidant activity in commercial varieties of tomato (Lycopersicum esculentum), J. Sci. Food Agric. 82 (2002) 323–330, https://doi.org/10.1002/ jsfa.1035.
- [77] C.-H. Liu, L.-Y. Cai, X.-Y. Lu, X.-X. Han, Y. Tie-Jin, Effect of Postharvest UV-C Irradiation on Phenolic Compound Content and Antioxidant Activity of Tomato Fruit During Storage, J. Integr. Agric. 2012 (2012) 159–165.
- [78] B. Inbaraj, B. Chen, Carotenoids in Tomato Plants, in: Tomatoes and Tomato Products, Science Publishers, 2008: pp. 133–164. 10.1201/9781439843390-c7.
- [79] G. Cioffi, M.S. Pesca, P. de Caprariis, A. Braca, L. Severino, N. de Tommasi, Phenolic compounds in olive oil and olive pomace from Cilento (Campania, Italy) and their antioxidant activity, Food Chem. 121 (2010) 105–111, https://doi.org/ 10.1016/i.foodchem.2009.12.013.
- [80] M. Servili, S. Esposto, R. Fabiani, S. Urbani, A. Taticchi, F. Mariucci, R. Selvaggini, G.F. Montedoro, Phenolic compounds in olive oil: Antioxidant, health and organoleptic activities according to their chemical structure, Inflammopharmacology 17 (2009) 76–84, https://doi.org/10.1007/s10787-008-8014-y
- [81] C.R. Brown, Invited Review Antioxidants in Potato, Amer. J. Potato Res. 82 (2005) 163–172, https://doi.org/10.1007/BF02853654.

- [82] P. *Pinsirodom, P. Taprap, R. Parinyapatthanaboot, Antioxidant activity and phenolic acid composition in different parts of selected cultivars of mangoes in Thailand, Int. Food Res. J. 25 (2018) 1435–1443.
- [83] MarketWatch, Ascorbic Acid Market Global Size Analysis 2021: Growth Analysis by Top Manufacturers, Market Specific Business Developments, Top Grooming Regions, Future Prospects with Covid-19 Impact Forecast to 2027, (2022).
- [84] Gallic Acid Market Size Worth 71 million USD at a CAGR of 2.4% L Top Countries Data, Analysis by Trends, Growth and Forecast 2021- 2026, MarketWatch. (2021).
- [85] Global Vanillic Acid (CAS 121-34-6) Market by Type (Purity Greater than or equal to99%, Purity 98%), By Application (Pharmaceutical Intermediates, Flavors & Fragrances, Other) And By Region (North America, Latin America, Europe, Asia Pacific and Middle East & Africa), Forecast From 2022 To 2030, MarketWatch. (2020). https://industrygrowthinsights.com/report/vanillic-acid-market/.
- [86] Global Beta Carotene Market Size, Market Share, Application Analysis, Regional Outlook, Growth Trends, Key Players, Competitive Strategies and Forecasts, 2017 -2025, Business Wire. (2017).
- [87] Market Growth Reports, Chlorogenic Acid Market Size In 2022: New Technological Trend & Development with Top Key Players, Industry Analysis by Top Manufactures, Product Demand Forecast Till 2026, The Express Wire. (2022). https://www.marketwatch.com/press-release/chlorogenic-acid-market-size-in-20 22-new-technological-trend-development-with-top-key-players-industry-analysisby-top-manufactures-product-demand-forecast-till-2026-124-report-pages-2022-0 8-09 (accessed October 31, 2022).

- [88] Ferulic Acid Market (By Type: Synthesis, Natural; By Application: Cosmetic, Pharmaceutical Intermediates, Others; By Packaging: Interior Packaging, Exterior Packaging) - Global Industry Analysis, Size, Share, Growth, Trends, Regional Outlook, and Forecast 2022-2030, Precedence Research (2022). https://www. precedenceresearch.com/ferulic-acid-market.
- [89] Quercetin Market Size, Share & Trends Analysis Report By Type (Food Grade, Reagent/Chemical Grade, Others) By Nature (Organic, Conventional) By End Uses (Food & Beverage Industry, Pharmaceutical, Dietary Supplement & Nutraceutical, Others) Based On Region, And Segment Forecasts, 2021-2027, BMRC 1755, Brand Essence Research (2021).
- [90] Kaempferol Market Demand, Share, Forecast to 2030, Straits Research. (2022). htt ps://straitsresearch.com/report/kaempferol-market (accessed March 31, 2023).

Further reading

- [11] M.A.M. Ali, R.M. Yunus, C.K. Cheng, J. Gimbun, Successive optimisation of waste cooking oil transesterification in a continuous microwave assisted reactor, RSC Adv. 5 (2015) 76743–76751, https://doi.org/10.1039/c5ra15834f.
- [67] P.B. Pagès, F. Le Pimpec-Barthes, A. Bernard, Chirurgie des métastases pulmonaires des cancers colorectaux: facteurs prédictifs de survie, Rev. Mal. Respir. 33 (2016) 838–852, https://doi.org/10.1016/j.rmr.2016.02.006.